arXiv:q-bio/0502035v1 [q-bio.MN] 23 Feb 2005

# Functional cartography of complex metabolic networks

Roger Guimerà and Luís A. Nunes Amaral

NICO and Dept. Chemical and Biological Engineering

Northwestern University, Evanston, IL 60208, USA

**High-throughput techniques are leading to an explosive growth in the size of biological databases and creating the opportunity to revolutionize our understanding of life and disease. Interpretation of these data remains, however, a major scientific challenge. Here, we propose a methodology that enables us to extract and display information contained in complex networks[1,2,3]. Specifically, we demonstrate that one can (i) find functional modules[4,5] in complex networks, and (ii) classify nodes into universal roles according to their pattern of intra- and inter-module connections. The method thus yields a "cartographic representation" of complex networks. Metabolic networks[6,7,8] are among the most challenging biological networks and, arguably, the ones with more potential for immediate applicability[9]. We use our method to analyze the metabolic networks of twelve organisms from three different super-kingdoms. We find that, typically, 80% of the nodes are only connected to other nodes within their respective modules, and that nodes with different roles are affected by different evolutionary constraints and pressures. Remarkably, we**

**find that low-degree metabolites that connect different modules are more conserved than hubs whose links are mostly within a single module.**

If one is to extract the significant information from the topology of a large complex network, the knowledge of the role of each node is of crucial importance. A cartographic analogy is helpful to illustrate this point. Consider the network formed by all cities and towns in a country—the nodes—and all the roads that connect them—the links. It is clear that a map in which each city and town is represented by a circle of fixed size and each road is represented by a line of fixed width is hardly useful. Rather, real maps emphasize capitals and important communication lines so that one can obtain scale-specific information at a glance. Similarly, it is difficult, if not impossible, to obtain information from a network with hundreds or thousands of nodes and links, unless the information about nodes and links is conveniently summarized. This is particularly true for biological networks.

Here, we propose a methodology, which is based on the connectivity of the nodes, that yields a "cartographic representation" of a complex network. The first step in our method is to identify the functional modules[4,5] in the network. In the cartographic picture, modules are analogous to countries or regions, and enable a coarse-grained, and thus simplified, description of the network. Then, we classify the nodes in the network into a small number of *system-independent* "universal roles."

*Modules.* It is a matter of common experience that social networks have communities of highly interconnected nodes that are less connected to nodes in other communities. Such modular structures have been reported not only in social networks[5,10,11,12], but also in food webs[13] and biochemical networks[4,14,15,16]. It is widely believed that the modular structure of complex networks plays a critical role in their functionality[4,14,16]. There is therefore a clear need to develop algorithms to identify modules accurately[5,11,17,18,19,20].

We identify modules by maximizing the network's *modularity*[11,18,21] using simulated annealing[22] (see Methods). Simulated annealing enables us to carry out an exhaustive search and to minimize the problem of finding sub-optimal partitions. It is noteworthy that, in our method,

one does not need to specify a priori the number of modules; rather, this number is an outcome of the algorithm. Our algorithm, which significantly outperforms the best algorithm in the literature, is able to reliably identify modules in a network whose nodes have as many as 50% of their connections outside their own module (Fig. 1).

*Roles in modular networks.* It is plausible to surmise that the nodes in a network are connected according to the *role* they fulfill. This fact has been long recognized in the analysis of social networks[23]. For example, in a classical hierarchical organization, the CEO is not directly connected to plant employees but is connected to the members of the board of directors. Importantly, such a statement holds for virtually any organization, that is, the role of CEO is defined irrespective of the particular organization one considers.

We propose a new method to determine the role of a node in a complex network. Our approach is based on the idea that nodes with the same role should have similar topological properties[24] (see Supplementary Information for a discussion on how our approach relates to previous work). We hypothesize that the role of a node can be determined, to a great extent, by its *within-module degree* and its *participation coefficient*, which define how the node is positioned in its own module and with respect to other modules[25,26] (see Methods). These two properties are easily computed once the modules of a network are known.

The within-module degree $z_i$ measures how "well-connected" node $i$ is to other nodes in the module. High values of $z_i$ indicate high within-module degrees and vice versa. The participation coefficient $P_i$ measures how "well-distributed" the links of node $i$ are among different modules. The participation coefficient $P_i$ is close to one if its links are uniformly distributed among all the modules and zero if all its links are within its own module.

We define heuristically seven different "universal roles," each defined by a different region in the $zP$ parameters-space (Fig. 2). According to the within-module degree, we classify nodes with $z \geq 2.5$ as module hubs and nodes $z < 2.5$ as non-hubs. Both hub and non-hub nodes are then more finely characterized by using the values of the participation coefficient (see Supplementary Information for a detailed justification of this classification scheme, and for a

discussion on possible alternatives).

We find that non-hub nodes can be naturally divided into four different roles: (R1) *ultra-peripheral nodes*, i.e., nodes with all its links within their module ($P \leq 0.05$); (R2) *peripheral nodes*, i.e., nodes with most links within their module ($0.05 < P \leq 0.62$); (R3) *non-hub connector nodes*, i.e., nodes with many links to other modules ($0.62 < P \leq 0.80$); and (R4) *non-hub kinless nodes*, i.e., nodes with links homogeneously distributed among all modules ($P > 0.80$). We find that hub nodes can be naturally divided into three different roles: (R5) *provincial hubs*. i.e., hub nodes with the vast majority of links within their module ($P \leq 0.30$); (R6) *connector hubs*, i.e., hubs with many links to most of the other modules ($0.30 < P \leq 0.75$); and (R7) *kinless hubs*, i.e., hubs with links homogeneously distributed among all modules ($P > 0.75$).

*Cartographic representation of metabolic networks.* To test the applicability of our approach to complex biological networks, we consider the metabolic network[6,7,14,8,9] of twelve organisms: four bacteria (*E. coli*, *B. subtilis*, *L. lactis*, and *T. elongatus*), four eukaryotes (*S. cerevisiae*, *C. elegans*, *P. falciparum*, and *H. sapiens*), and four archaea (*P. furiosus*, *A. pernix*, *A. fulgidus*, and *S. solfataricus*). In metabolic networks, nodes represent metabolites and two nodes $i$ and $j$ are connected by a link if there is a chemical reaction in which $i$ is a substrate and $j$ a product, or vice versa. In our analysis, we use the database developed by Ma and Zeng[8] (MZ) from the Kyoto Encyclopedia of Genes and Genomes[27] (KEGG). Importantly, the results we report are not altered if we consider the complete KEGG database instead (Figs. 2c and 4b, and Supplementary Information).

First, we identify the functional modules in the different metabolic networks (Fig. 3). Finding modules in metabolic networks based on purely topological properties is an extremely important task. For example, Schuster *et al.* have reported on the impossibility of obtaining elementary flux modes[28] from complete metabolic networks due to the combinatorial explosion of the number of such modes[29]. Our algorithm identifies an average of 15 different modules in each metabolic network—with a maximum of 19 for *E. coli* and *H. sapiens*, and a minimum of

11 for *A. fulgidus*. As expected, the density of links within each of the modules is significantly larger than between modules, typically 100-1000 times larger (see Supplementary Information).

To assess how each of the modules is related to the pathways traditionally defined in biology, we use the classification scheme proposed in KEGG, which includes nine major pathways: carbohydrate metabolism, energy metabolism, lipid metabolism, nucleotide metabolism, amino acid metabolism, glycan biosynthesis and metabolism, metabolism of cofactors and vitamins, biosynthesis of secondary metabolites, and biodegradation of xenobiotics. Each metabolite in the KEGG database is assigned to, at least, one pathway; thus, we can determine to which pathways the metabolites in a given module belong. We find that most modules contain metabolites mostly from one major pathway. For example, in 17 of the 19 modules identified for *E. coli*, more than one third of the metabolites belong to a single pathway. Interestingly, some other modules—two in the case of *E. coli*—cannot be trivially associated with a single traditional pathway. These modules are typically central in the metabolism and contain, mostly, metabolites that are classified in KEGG as belonging to carbohydrate and amino acid metabolism.

Next, we identify the role of each metabolite. In Fig. 2b we show the roles identified in the metabolic network of *E. coli*. Remarkably, other organisms display a similar distribution of the nodes in the different roles, even though they correspond to organisms that are very distant from an evolutionary standpoint (see Supplementary Information). Role R1, which contains ultra-peripheral metabolites with small degree and no between-module links, comprises 76-86% of all the metabolites in the networks. This considerably simplifies the coarse-grained representation of the network as these nodes do not need to be identified separately. Note that this finding alone represents an important step towards the goal of extracting scale-specific information from complex networks.

*Metabolite role and inter-species conservation.* The information about modules and roles enables us to build a "cartographic representation" of the metabolic network of, for example, *E. coli* (Fig. 3). This representation enables us to recover relevant biological information. For instance, we find that the metabolism is mostly organized around the module containing pyru-

vate, which, in turn, is strongly connected to the module whose hub is acetyl-CoA. These two molecules are key to connect the metabolism of carbohydrates, amino acids, and lipids to the TCA cycle from which ATP is obtained. These two modules are connected to more peripheral ones by key metabolites such as D-glyceraldehyde 3-phosphate and D-fructose 6-phosphate (which connect to the glucose and galactose metabolisms), D-ribose 5-phosphate (which connects to the metabolism of certain nucleotides), and glycerone phosphate (which connects to the metabolism of certain lipids).

Importantly, our analysis also uncovers nodes with key connector roles that take part in only a small but fundamental set of reactions. For example, N-carbamoyl-L-aspartate takes part in only three reactions but is vital because it connects the pyrimidine metabolism, whose hub is uracil, to the core of the metabolism through the alanine and aspartate metabolism. The potential importance of such non-hub connectors points to another consideration. It is a plausible *hypothesis* that nodes with different roles are under different evolutionary constraints and pressures. In particular, one expects that nodes with structurally relevant roles are more necessary and therefore more conserved across species.

To quantify the relation between roles and conservation, we define the loss rate $p_{\rm lost}(R)$ (see Methods). Structurally relevant roles are expected to have low values of $p_{\rm lost}(R)$ and vice versa. Remarkably, we find that the different roles have, indeed, different loss rates (Fig. 4). As expected, ultra-peripheral nodes (role R1) have the highest loss rate while connector hubs (role R6) are the most conserved across all species considered.

The results for the comparison of $p_{\rm lost}(R)$ for ultra-peripheral nodes and connector hubs is illustrative, but hardly surprising. The comparison of $p_{\rm lost}(R)$ for non-hub connectors (role R3) and provincial hubs (role R5), however, yields a surprising and remarkable finding. The metabolites in the provincial hubs class have many within-module connections, sometimes as much as five standard deviations more connections than the average node in the module. Conversely, non-hub connector metabolites have few links relative to other nodes in their modules—and fewer total connections than the metabolites in role R5 (see Supplementary Figs. S12b,c). The

links of non-hub connectors, however, are distributed among *several different modules*, while the links of provincial hubs are mainly within their modules. We find that non-hub connectors are systematically and significantly more conserved than provincial hub metabolites (Fig. 4).

A possible explanation for the high degree of conservation of non-hub connectors is the following. Connector nodes are responsible for inter-module fluxes. These modules are, otherwise, poorly connected or not connected at all to each other, so the elimination of connector metabolites will likely have a large impact on the global structure of fluxes in the network. On the contrary, the pathways in which provincial hubs are involved may be backed up within the module, in such a way that elimination of these metabolites may have a comparatively smaller impact, which, in addition, would likely be confined to the module containing the provincial hub.

Our results therefore point to the need to consider each complex biological network as a whole, instead of focusing on local properties. In protein networks, for example, it has been reported that hubs are more essential than non-hubs[30]. Notwithstanding the relevance of such a finding, our results suggest that the global role of nodes in the network might be a better indicator of their importance than degree[26].

Our "cartography" provides a scale-specific method to process the information contained in the structure of complex networks, and to extract knowledge about the function carried out by the network and its constituents. An open question is how to adapt current module-detection algorithms to networks with a hierarchical structure.

For metabolic networks, a comparatively well studied and well understood case, our method allows us to recover firmly established biological facts, and to uncover important new results, such as the significant conservation of non-hub connector metabolites. Similar results can be expected when our method is applied to other complex networks that are not as well studied as metabolic networks. Among those, protein interaction and gene regulation networks may be the most significant.

# Methods

## Modularity

For a given partition of the nodes of a network into modules, the modularity $M$ of this partition is[11,18,21]

$$M \equiv \sum_{s=1}^{N_M} \left[ \frac{l_s}{L} - \left( \frac{d_s}{2L} \right)^2 \right] , \quad (1)$$

where $N_M$ is the number of modules, $L$ is the number of links in the network, $l_s$ is the number of links between nodes in module $s$, and $d_s$ is the sum of the degrees of the nodes in module $s$. The rationale for this definition of modularity is the following. A good partition of a network into modules must comprise many within-module links and as few as possible between-module links. However, if one just tries to minimize the number of between-module links (or, equivalently, maximize the number of within-module links) the optimal partition consists of a single module and no between-module links. Equation (1) addresses this difficulty by imposing that $M = 0$ if nodes are placed at random into modules *or* if all nodes are in the same cluster[11,18,21].

The objective of a module identification algorithm is to find the partition with largest modularity, and several methods have been proposed to attain such a goal. Most of them rely on heuristic procedures and use $M$—or a similar measure—only to assess their performance. In contrast, we use simulated annealing[22] to find the partition with the largest modularity.

## Simulated annealing for module identification

Simulated annealing[22] is a stochastic optimization technique that enables one to find "low cost" configurations without getting trapped in "high-cost" local minima. This is achieved by introducing a *computational temperature* $T$. When $T$ is high, the system can explore configurations of high cost while at low $T$ the system only explores low cost regions. By starting at high $T$ and slowly decreasing $T$, the system descends gradually toward deep minima, eventually overcoming small cost barriers.

When identifying modules, the objective is to maximize the modularity and, thus, the cost is $C = -M$, where $M$ is the modularity as defined in Eq. (1). At each temperature, we perform a number of random updates and accept them with probability

$$p = \begin{cases} 1 & \text{if} \quad C_f \leq C_i \\ \exp\left(-\frac{C_f - C_i}{T}\right) & \text{if} \quad C_f > C_i \end{cases} \tag{2}$$

where $C_f$ is the cost after the update and $C_i$ is the cost before the update.

Specifically, at each $T$ we propose $n_i = fS^2$ individual node movements from one module to another, where $S$ is the number of nodes in the network. We also propose $n_c = fS$ collective movements, which involve either the merging two modules or splitting a module. For $f$ we typically choose $f = 1$. After the movements are evaluated at a certain $T$, the system is cooled down to $T' = cT$, with $c = 0.995$.

## Within-module degree and participation coefficient

Each module can be organized in very different ways, ranging from totally centralized—with one or a few nodes connected to all the others—to totally decentralized—with all nodes having similar connectivities. Nodes with similar roles are expected to have similar relative within-module connectivity. If $\kappa_i$ is the number of links of node $i$ to other nodes in its module $s_i$, $\overline{\kappa}_{s_i}$ is the average of $\kappa$ over all the nodes in $s_i$, and $\sigma_{\kappa_{s_i}}$ is the standard deviation of $\kappa$ in $s_i$, then

$$z_i = \frac{\kappa_i - \overline{\kappa}_{s_i}}{\sigma_{\kappa_{s_i}}} \tag{3}$$

is the so-called $z$-score. The within-module degree $z$-score measures how "well-connected" node $i$ is to other nodes in the module.

Different roles can also arise because of the connections of a node to modules other than its own. For example, two nodes with the same $z$-score will play different roles if one of them is connected to several nodes in other modules while the other is not. We define the participation coefficient $P_i$ of node $i$ as

$$P_i = 1 - \sum_{s=1}^{N_M} \left(\frac{\kappa_{is}}{k_i}\right)^2 \tag{4}$$

where $\kappa_{is}$ is the number of links of node $i$ to nodes in module $s$, and $k_i$ is the total degree of node $i$. The participation coefficient of a node is therefore close to one if its links are uniformly distributed among all the modules and zero if all its links are within its own module.

### Loss rate

To quantify the relation between roles and conservation, we calculate to which extent metabolites are conserved in the different species depending on the role they play. Specifically, for a pair of species, $A$ and $B$, we define the loss rate as the probability $p(R_A = 0|R_B = R) \equiv p_{\rm lost}(R)$ that a metabolite is not present in one of the species ($R_A = 0$) given that it plays role $R$ in the other species ($R_B = R$). Structurally relevant roles are expected to have low values of $p_{\rm lost}(R)$ and vice versa.

## References


1. Amaral, L. A. N., Scala, A., Barthelémy, M. & Stanley, H. E. Classes of small-world networks. *Proc. Natl. Acad. Sci. USA* **97**, 11149–11152 (2000).

2. Albert, R. & Barabási, A.-L. Statistical mechanics of complex networks. *Rev. Mod. Phys.* **74**, 47–97 (2002).

3. Amaral, L. A. N. & Ottino, J. Complex networks: Augmenting the framework for the study of complex systems. *Eur. Phys. J. B* **38**, 147–162 (2004).

4. Hartwell, L. H., Hopfield, J. J., Leibler, S. & Murray, A. W. From molecular to modular biology. *Nature* **402**, C47–C52 (1999).

5. Girvan, M. & Newman, M. E. J. Community structure in social and biological networks. *Proc. Natl. Acad. Sci. USA* **99**, 7821–7826 (2002).

6. Jeong, H., Tombor, B., Albert, R., Oltvai, Z. N. & Barabási, A. L. The large-scale organization of metabolic networks. *Nature* **407**, 651–654 (2000).

7. Wagner, A. & Fell, D. A. The small world inside large metabolical networks. *Proc. Roy. Soc. B* **268**, 1803–1810 (2001).

8. Ma, H. & Zeng, A.-P. Reconstruction of metabolic networks from genome data and analysis of their global structure for various organisms. *Bioinformatics* **19**, 270–277 (2003).

9. Hatzimanikatis, V., Li, C., Ionita, J. A. & Broadbelt, L. Metabolic networks: enzyme function and metabolite structure. *Curr. Opin. Struc. Biol.* **14**, 300–306 (2004).

10. Guimerà, R., Danon, L., Díaz-Guilera, A., Giralt, F. & Arenas, A. Self-similar community structure in a network of human interactions. *Phys. Rev. E* **68**, art. no. 065103 (2003).

11. Newman, M. E. J. & Girvan, M. Finding and evaluating community structure in networks. *Phys. Rev. E* **69**, art. no. 026113 (2004).

12. Arenas, A., Danon, L., Díaz-Guilera, A., Gleiser, P. M. & Guimerà, R. Community analysis in social networks. *Eur. Phys. J. B* **38**, 373–380 (2004).

13. Krause, A. E., Frank, K. A., Mason, D. M., Ulanowicz, R. E. & Taylor, W. W. Compartments revealed in food-web structure. *Nature* **426**, 282–285 (2003).

14. Ravasz, E., Somera, A. L., Mongru, D. A., Oltvai, Z. N. & Barabási, A.-L. Hierarchical organization of modularity in metabolic networks. *Science* **297**, 1551–1555 (2002).

15. Holme, P. & Huss, M. Subnetwork hierarchies of biochemical pathways. *Bioinformatics* **19**, 532–538 (2003).

16. Papin, J. A., Reed, J. L. & Palsson, B. O. Hierarchical thinking in network biology: the unbiased modularization of biochemical networks. *Trends Biochem. Sci.* **29**, 641–647 (2004).

17. Eriksen, K. A., Simonsen, I., Maslov, S. & Sneppen, K. Modularity and extreme edges of the Internet. *Phys. Rev. Lett.* **90**, art. no. 148701 (2003).

18. Newman, M. E. J. Fast algorithm for detecting community structure in networks. *Phys. Rev. E* **69**, art. no. 066133 (2004).

19. Radicchi, F., Castellano, C., Cecconi, F., Loreto, V. & Parisi, D. Defining and identifying communities in networks. *Proc. Natl. Acad. Sci. USA* **101**, 2658–2663 (2004).

20. Donetti, L. & Muñoz, M. A. Detecting network communities: A new systematic and efficient algorithm. *J. Stat. Mech. Theor. Exp.* P10012 (2004).

21. Guimerà, R., Sales-Pardo, M. & Amaral, L. A. N. Modularity from fluctuations in random graphs and complex networks. *Phys. Rev. E* **70**, art. no. 025101 (2004).

22. Kirkpatrick, S., Gelatt, C. D. & Vecchi, M. P. Optimization by simulated annealing. *Science* **220**, 671–680 (1983).

23. Wasserman, S. & Faust, K. *Social Network Analysis* (Cambridge University Press, Cambridge, U.K., 1994).

24. Guimerà, R. & Amaral, L. A. N. *J. Stat. Mech. Theor. Exp.* submitted (2004).

25. Rives, A. W. & Galitski, T. Modular organization of cellular networks. *Proc. Natl. Acad. Sci. USA* **100**, 1128–1133 (2003).

26. Han, J.-D. J. *et al.* Evidence for dinamically organized modularity in the yeast protein-protein interaction network. *Nature* **430**, 88–93 (2004).

27. Kanehisa, M. & Goto, S. KEGG: Kyoto Encyclopedia of Genes and Genomes. *Nucleic Acids Res.* **28**, 27–30 (2000).

28. Schuster, S., Fell, D. A. & Dandekar, T. A general definition of metabolic pathways useful for systematic organization and analysis of complex metabolic networks. *Nat. Biotechnol.* **18**, 326–332 (2000).

29. Schuster, S., Pfeiffer, T., Moldenhauer, F., Koch, I. & Dandekar, T. Exploring the pathway structure of metabolism: decomposition into subnetworks and application to *Microplasma pneumoniae*. *Bioinformatics* **18**, 351–361 (2002).

30. Jeong, H., Mason, S. P., Barabási, A.-L. & Oltvai, Z. N. Lethality and centrality in protein networks. *Nature* 41–42 (2001).

**Acknowledgments** We thank L. Broadbelt, V. Hatzimanikatis, A. A. Moreira, E. T. Papoutsakis, M. Sales-Pardo, and D. B. Stouffer for stimulating discussions and helpful suggestions, and H. Ma and A. P. Zeng for providing us with their metabolic networks' database. R.G. thanks the Fulbright Program and the Spanish Ministry of Education, Culture & Sports. L.A.N.A. gratefully acknowledges the support of a Searle Leadership Fund Award and of a NIH/NIGMS K-25 award.

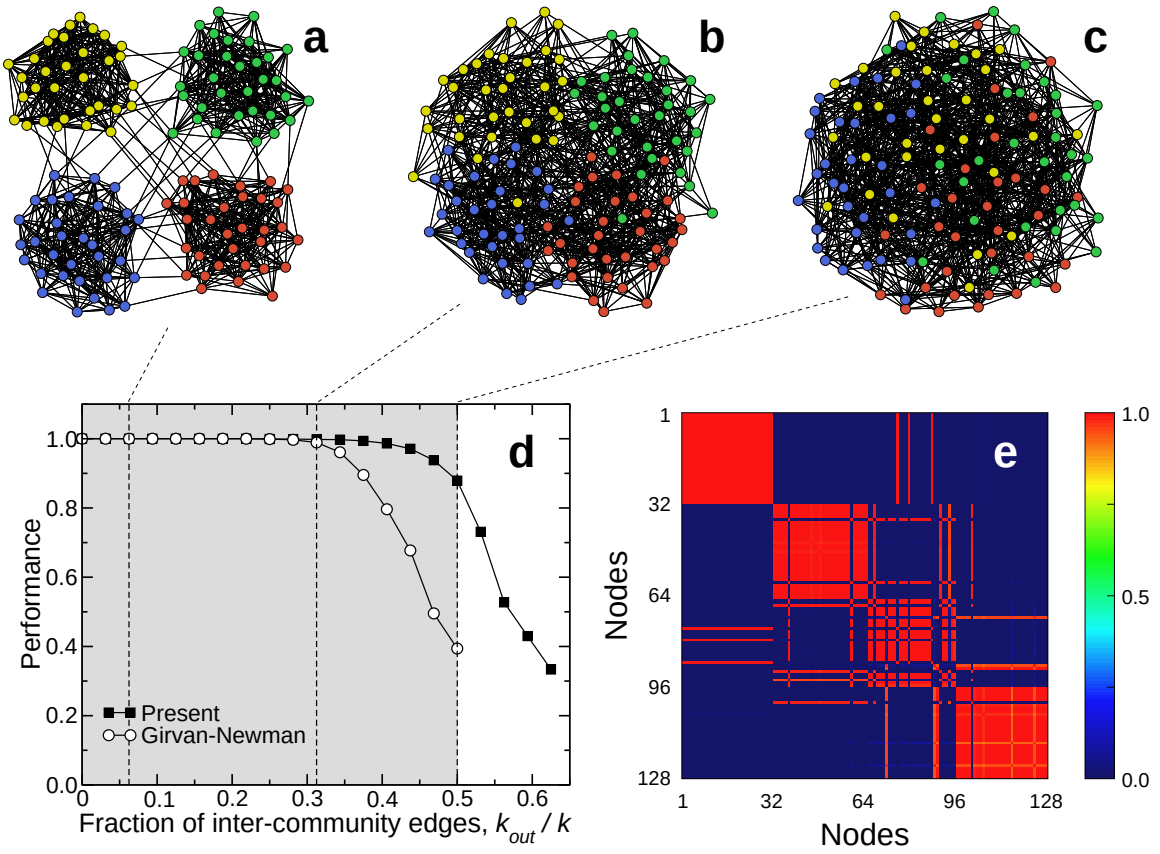



Figure 1: Performance of module identification methods. To test the performance of the method, we build "random networks" with known module structure. Each test network comprises 128 nodes divided into 4 modules of 32 nodes. Each node is connected to the other nodes in its module with probability $p_i$, and to nodes in other modules with probability $p_o < p_i$. On average, thus, each node is connected to $k_{out} = 96\,p_o$ nodes in other modules and to $k_{in} = 31\,p_i$ in the same module. Additionally, $p_i$ and $p_o$ are selected so that the average degree of the nodes is $k = 16$. We display networks with: **a,** $k_{in} = 15$ and $k_{out} = 1$; **b,** $k_{in} = 11$ and $k_{out} = 5$; and **c,** $k_{in} = k_{out} = 8$. **d,** The performance of a module identification algorithm is typically defined as the fraction of correctly classified nodes. We compare our algorithm to the Girvan-Newman algorithm[5,18], which is the reference algorithm for module identification [11,18,19]. Note that our method is 90% accurate even when half of a node's links are to nodes in outside modules. **e,** Our module-identification algorithm is stochastic, so different runs yield, in principle, different partitions. To test the robustness of the algorithm, we obtain 100 partitions of the network depicted in **c** and plot, for each pair of nodes in the network, the fraction of times that they are classified in the same module. As shown in the figure, most pairs of nodes are either always classified in the same module (red) or never classified in the same module (dark blue), which indicates that the solution is robust.

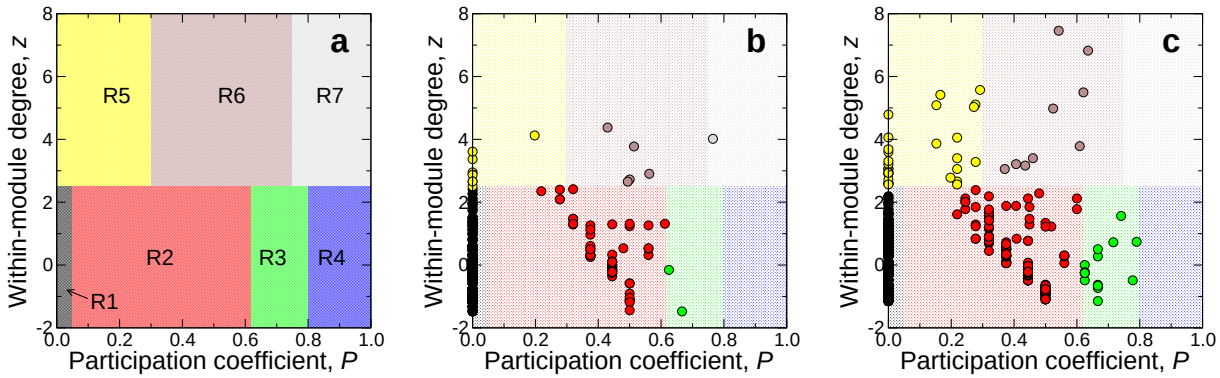



Figure 2: Roles and regions in the $zP$ parameters-space. **a,** Each node in a network can be characterized by its within-module degree and its participation coefficient (see Methods for definitions.) We classify nodes with $z \geq 2.5$ as module hubs and nodes $z < 2.5$ as non-hubs. We find that non-hub nodes can be naturally assigned into four different roles: (R1) *ultra-peripheral nodes*, i.e., nodes with all its links within their module; (R2) *peripheral nodes*, i.e., nodes with most links within their module; (R3) *non-hub connector nodes*, i.e., nodes with many links to other modules; and (R4) *non-hub kinless nodes*, i.e., nodes with links homogeneously distributed among all modules. We find that hub nodes can be naturally assigned into three different roles: (R5) *provincial hubs*. i.e., hub nodes with the vast majority of links within their module; (R6) *connector hubs*, i.e., hubs with many links to most of the other modules; and (R7) *kinless hubs*, i.e., hubs with links homogeneously distributed among all modules. (Supplementary Information.) **b,** Metabolite role determination for the metabolic network *E. coli*, as obtained from the MZ database. Each metabolite is represented as a point in the $zP$ parameters-space, and is colored according to its role. **c,** Same as **b** but for the complete KEGG database.

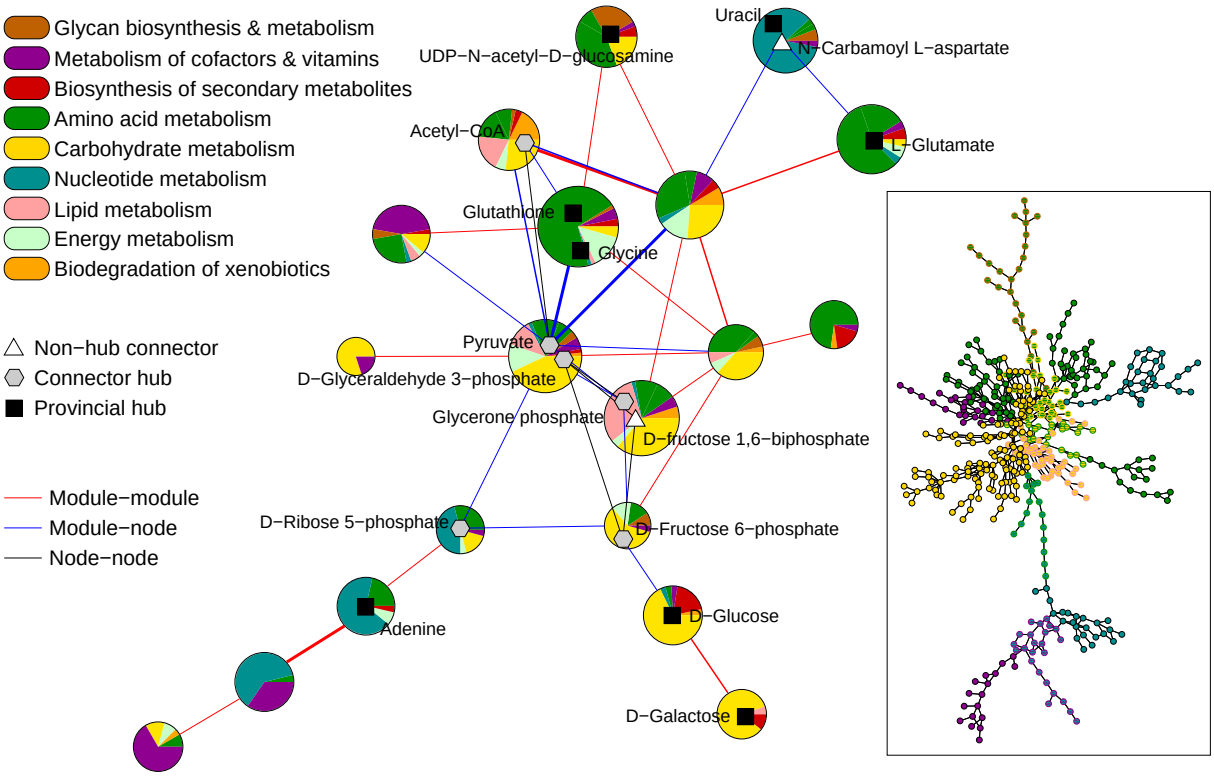



Figure 3: "Cartographic representation" of the metabolic network of *E. coli*. Each circle represents a module and is colored according to the KEGG pathway classification of the metabolites it contains. Certain important nodes are depicted as triangles (non-hub connectors), hexagons (connector hubs), and squares (provincial hubs). Interactions between modules and nodes are depicted using lines, whith thickness proportional to the number of actual links. (Inset) Pajek-obtained representation of the entire metabolic network of *E. coli* contains 473 metabolites and 574 links. Each node is colored according to the "main" color of its module, as obtained from the "cartographic representation."

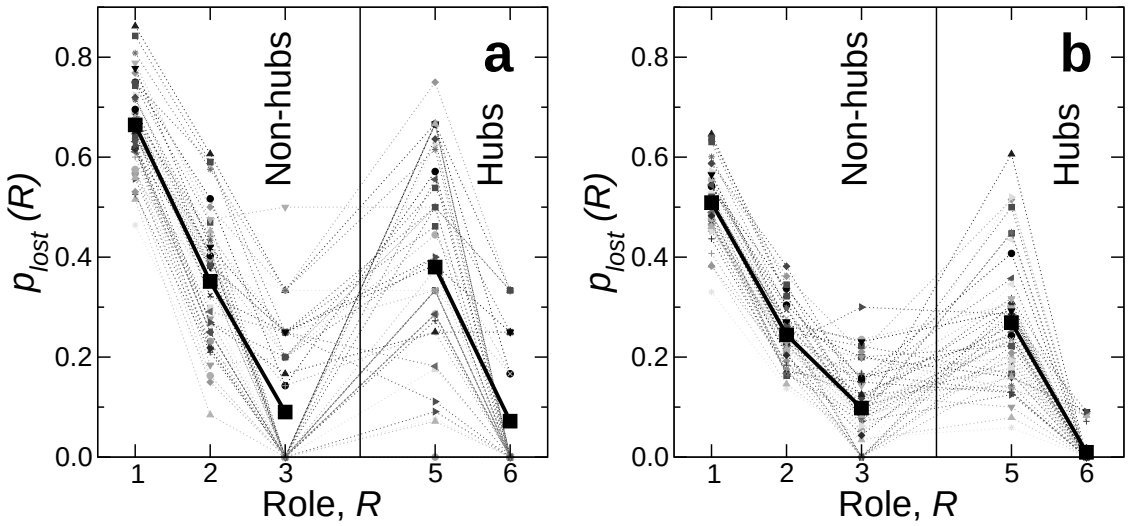



Figure 4: Roles of metabolites and inter-species conservation. To quantify the relation between roles and conservation, we calculate the loss rate $p_{\rm lost}(R)$ of each metabolite (see Methods). Each thin line in the graph corresponds to a comparison between two species. Since we are interested in metabolites that are present in some species but missing in others, metabolic networks of species within the same super-kingdom—bacteria, eukaryotes, and archaea—are usually too similar to provide statistically sound information, especially for roles containing only a few metabolites. Therefore, we consider in our analysis only pairs of species that belong to different super-kingdoms. The thick line is the average over all pairs of species. The loss rate $p_{\rm lost}(R)$ is maximum for ultra-peripheral (R1) nodes and minimum for connector hubs (R6). Remarkably, provincial hubs (R5) have a significantly and consistently higher $p_{\rm lost}(R)$ than non-hub connectors (R3), even though the within-module degree and the total degree of provincial hubs is larger. Note that, out of the total 48 pair comparisons, only in two cases $p_{\rm lost}(R)$ is lower for provincial hubs than for non-hub connectors, while the opposite is true in 44 cases. **a,** Results obtained for the MZ database and **b,** the complete KEGG database.